New Journal of Physics
The open access journal at the forefront of physics

Deutsche Physikalische Gesellschaft DPG IOP Institute of Physics

PAPER • OPEN ACCESS

Stochastic spin flips in polariton condensates: nonlinear tuning from GHz to sub-Hz

To cite this article: Yago del Valle-Inclan Redondo *et al* 2018 *New J. Phys.* **20** 075008

New Journal of Physics
The open access journal at the forefront of physics

Deutsche Physikalische Gesellschaft DPG
IOP Institute of Physics

Published in partnership with: Deutsche Physikalische Gesellschaft and the Institute of Physics

CrossMark

OPEN ACCESS

PUBLISHED
21 August 2018

ERRATUM

Erratum: Stochastic spin flips in polariton condensates: nonlinear tuning from GHz to sub-Hz (2018 *New J. Phys.* 20 075008)

Yago del Valle-Inclan Redondo[1,9], Hamid Ohadi[1,2], Yuri G Rubo[3,4], Orr Beer[1], Andrew J Ramsay[5], Symeon I Tsintzos[6], Zacharias Hatzopoulos[6], Pavlos G Savvidis[6,7,8] and Jeremy J Baumberg[1]

[1] NanoPhotonics Centre, Department of Physics, Cavendish Laboratory, University of Cambridge, Cambridge CB3 0HE, United Kingdom
[2] SUPA, School of Physics and Astronomy, University of St Andrews, St Andrews KY16 9SS, United Kingdom
[3] Instituto de Energías Renovables, Universidad Nacional Autónoma de México, Temixco, Morelos 62580, Mexico
[4] Center for Theoretical Physics of Complex Systems, Institute for Basic Science (IBS), Daejeon 34051, Republic of Korea
[5] Hitachi Cambridge Laboratory, Hitachi Europe Ltd, Cambridge CB3 0HE, United Kingdom
[6] Microelectronics Research Group, IESL-FORTH, Institute of Electronic Structure and Laser, 71110 Heraklion, Crete, Greece
[7] Department of Materials Science and Technology, University of Crete, 71110 Heraklion, Crete, Greece
[8] SOLAB, St. Petersburg State University, 198504 St. Petersburg, Russia
[9] Author to whom any correspondence should be addressed.

Due to an error in the production process, Γ was changed to Gcy in equation (1). The correct equation should read:

$$\frac{\mathrm{d}n_+}{\mathrm{d}t} = P - \Gamma_x n_+ - R_s\,|\psi_+|^2 n_+ - R_o\,|\psi_-|^2 n_+,$$

$$\frac{\mathrm{d}n_-}{\mathrm{d}t} = P - \Gamma_x n_- - R_s\,|\psi_-|^2 n_- - R_o\,|\psi_+|^2 n_-,$$

$$\frac{\mathrm{d}\psi_+}{\mathrm{d}t} = \left[\frac{1}{2}(R_s n_+ + R_o n_- - \Gamma_p) - \frac{\mathrm{i}}{2}(\alpha_1\,|\psi_+|^2 + \alpha_2\,|\psi_-|^2)\right]\psi_+ - \frac{1}{2}(\gamma - \mathrm{i}\,\varepsilon)\psi_- + \sqrt{R_s n_+ + R_o n_-}\,\frac{\mathrm{d}W_+}{\mathrm{d}t},$$

$$\frac{\mathrm{d}\psi_-}{\mathrm{d}t} = \left[\frac{1}{2}(R_s n_- + R_o n_+ - \Gamma_p) - \frac{\mathrm{i}}{2}(\alpha_1\,|\psi_-|^2 + \alpha_2\,|\psi_+|^2)\right]\psi_- - \frac{1}{2}(\gamma - \mathrm{i}\,\varepsilon)\psi_+ + \sqrt{R_s n_- + R_o n_+}\,\frac{\mathrm{d}W_-}{\mathrm{d}t}$$

New Journal of Physics
The open access journal at the forefront of physics

Deutsche Physikalische Gesellschaft DPG
IOP Institute of Physics

Published in partnership with: Deutsche Physikalische Gesellschaft and the Institute of Physics

CrossMark

OPEN ACCESS

RECEIVED
17 November 2017

REVISED
8 June 2018

ACCEPTED FOR PUBLICATION
13 July 2018

PUBLISHED
26 July 2018

PAPER

Stochastic spin flips in polariton condensates: nonlinear tuning from GHz to sub-Hz

Yago del Valle-Inclan Redondo[1,9], **Hamid Ohadi**[1,2], **Yuri G Rubo**[3,4], **Orr Beer**[1], **Andrew J Ramsay**[5], **Symeon I Tsintzos**[6], **Zacharias Hatzopoulos**[6], **Pavlos G Savvidis**[6,7,8] **and Jeremy J Baumberg**[1]

[1] NanoPhotonics Centre, Department of Physics, Cavendish Laboratory, University of Cambridge, Cambridge CB3 0HE, United Kingdom
[2] SUPA, School of Physics and Astronomy, University of St Andrews, St Andrews KY16 9SS, United Kingdom
[3] Instituto de Energías Renovables, Universidad Nacional Autónoma de México, Temixco, Morelos 62580, Mexico
[4] Center for Theoretical Physics of Complex Systems, Institute for Basic Science (IBS), Daejeon 34051, Republic of Korea
[5] Hitachi Cambridge Laboratory, Hitachi Europe Ltd, Cambridge CB3 0HE, United Kingdom
[6] Microelectronics Research Group, IESL-FORTH, Institute of Electronic Structure and Laser, 71110 Heraklion, Crete, Greece
[7] Department of Materials Science and Technology, University of Crete, 71110 Heraklion, Crete, Greece
[8] SOLAB, St. Petersburg State University, 198504 St. Petersburg, Russia
[9] Author to whom any correspondence should be addressed.

E-mail: ho35@st-andrews.ac.uk **and** jjb12@cam.ac.uk

Keywords: exciton–polariton, spin dynamics, non-equilibrium condensate, driven-dissipative, chaos

Abstract

The stability of spin of macroscopic quantum states to intrinsic noise is studied for non-resonantly-pumped optically-trapped polariton condensates. We demonstrate flipping between the two spin-polarised states with $>10^4$ slow-down of the flip rate by tuning the optical pump power. Individual spin flips faster than 50 ps are time resolved using single-shot streak camera imaging. We reproduce our results within a mean-field model accounting for cross-spin scattering between excitons and polaritons, yielding a ratio of cross- to co-spin scattering of ~0.6, in contrast with previous literature suggestions.

1. Introduction

Exciton–polaritons are light–matter excitations arising from the strong-coupling of photons and excitons in semiconductor microcavities [1]. Under non-resonant excitation, polaritons condense into a single quantum state and spontaneously develop macroscopic coherence [2]. This many-body state can be used to study different aspects of nonlinear dissipative many-body physics [3], with potential integration into optoelectronic devices [4, 5]. Developing ways of effectively trapping and controlling polariton condensates has been the subject of intense research [6–10]. Optical trapping methods are particularly flexible since they allow on-the-fly tuning of the condensate [11–13], and using spatially-patterned non-resonant pumps has proven to be a particularly simple and robust method. Using this technique, it is possible to create and control trapped polariton condensates [14–16], as well as larger arrays of condensates in which to study phase transitions in lattices [17, 18]. An unexpected result of this optical trapping is the observation of a parity-breaking symmetry bifurcation where the condensate spontaneously adopts a macroscopic spin and emits corresponding right- or left-circular polarisation [19], thanks to the reduced interactions with reservoir excitons. Nevertheless, fluctuations coming from the scattering of excitons into the condensate are an inherent internal source of noise for the polariton condensate [20–23].

Here we study the influence of this shot-noise on the stability of the circularly-polarised steady states of a trapped exciton–polariton condensate. We show that, under specific conditions, this noise is sufficiently large to destabilise the two steady-state macroscopic spins, leading to stochastic polarisation flipping dynamics. While stochastic formation of a polarised condensate has been reported before [23–25], the stochastic behaviour reported here occurs above the condensation threshold and is between two specific circularly polarised states, not the whole of the Poincare sphere.

We show that the condensate spin flip rate changes near-exponentially with pump power by four orders of magnitude, initially decreasing with power but increasing again at higher powers. This non-monotonous variation of the dwell time contrasts with a similar system based on vertical-cavity lasers where increasing power monotonously decreases their polarisation dwell time [26]. The unexpected power dependence of the spin-flip rate found here can only be explained by considering cross-spin scattering between the exciton reservoir and the polariton condensate. This adds a cross-spin gain saturation in the widely used mean-field models of polariton condensation [22, 27], and is needed to fully account for the spin degree of freedom of the exciton reservoir. We show numerically how this new term leads to an instability of the polarisation steady states at high pumping, which first leads to the formation of limit cycle polarisation oscillations and subsequently to chaotic behaviour due to limit cycle merging. These different polarisation steady states intuitively explain the experimentally-measured flip frequencies.

Finally, we use single-shot streak camera imaging to time-resolve individual spin flips. We observe that spin flips can occur with a wide range of timescales, even under the same experimental conditions. We measure spin flips to be at least as fast as 50 ps, of the same order of magnitude as the polariton lifetime. Combined with our experimental observation of 100 MHz spin flipping and with simulated spin flipping reaching 10 GHz, this puts a polariton random number generator (RNG) on a par with state-of-the-art laser diode systems [28].

2. Optically tuneable flip rate

We start by considering the spin flip dynamics of an individual optically-trapped polariton condensate. We use a $5\lambda/2$ GaAs microcavity ($Q > 16\,000$), with a detuning of -2 to -3 meV and Rabi splitting of 9 meV (details in [29]). Non-resonant pumping is achieved with a linearly-polarised continuous-wave laser (750 nm), chopped into 5 ms pulses using an acousto-optic modulator to avoid sample heating. Sample position, laser powers, and condensate densities are the same as those in [19]. The emitted light from the microcavity is filtered, polarisation-resolved and recorded with two photomultiplier tubes (PMTs) and a 5 GS s^{-1} (1 GHz) digital oscilloscope. The time resolution is here limited by the rise time of the PMT ($\sim$2 ns).

A spatial light modulator is used to shape the non-resonant laser into four diffraction-limited pump spots arranged in a 12 μm square. When focused on the semiconductor microcavity device, each pump spot creates a plasma of free carriers, blueshifting all the electronic energy levels through repulsive Coulomb interactions. The free carriers thermally relax, forming an exciton reservoir at the non-resonant laser spots. The exciton reservoir thermally relaxes, forming polaritons that accumulate at the bottom of the potential well inside the pump pattern [14, 19]. For appropriately chosen separations between the pump spots and sufficiently high powers (figure 1(a)), these polaritons form a macroscopically coherent state, with the polariton condensate trapped inside the pump spot potential (figure 1(b)) and remaining in the strong coupling regime (figure 1(c))[10].

These spatially-trapped condensates have been shown to exhibit a parity breaking transition with increasing power, where the initially-stable linearly-polarised condensate bifurcates into two circularly-polarised steady states, stochastically forming in one spin or its opposite every time it condenses [19]. This is also found to be the case here (figure 1(f)). The origin of these two parity-breaking states is closely related to self-trapping in coupled nonlinear modes and relies on energy and dissipation differences between two orthogonal linear modes of the polariton field, together with an asymmetry in the nonlinearity between spin-up and spin-down polaritons [19]. The fact that this bifurcation can be observed only with trapped condensates is a direct consequence of the spatial separation of the condensate and the exciton reservoir, leading to increased sensitivity of the polariton condensate to energy and dissipation inhomogeneities of the sample.

Here, despite spatial separation from the exciton reservoirs, we find that the two stable spin-polarised steady states can be destabilised due to random noise from reservoir pumping, leading to stochastic spin dynamics (figures 1(d), (e)). Above a critical bifurcation threshold ($P = 1.2P_{\mathrm{th}}$), we observe two nearly circularly polarised states (figure 1(f)). The magnitude of the spin (given by the degree of circular polarization of the emission) of the two spin-polarised states rapidly increases with power immediately after the bifurcation, followed by a slow decrease at even higher powers ($P > 1.7P_{\mathrm{th}}$). In addition to changes in the spin amplitude for the circularly-polarised states, we observe stochastic flipping between the two states (figures 1(d), (e)). By appropriately analysing this dynamic spin evolution, we extract the average flip rate at different powers (figure 1(g)). For pump powers just above the bifurcation threshold we observe a rapid decrease of the spin flip rate by more than four

[10] The particle number, $n = \Phi\tau|C|^{-2}$, where Φ is the photon flux, $\tau = 10$ ps is the polariton lifetime, and $|C|^2 = 0.4$ is the photon Hopfield coefficient. The photon flux is measured on a CCD using $\Phi = \alpha R/\eta$ where $\alpha = 3.5$ e^-/count is the photoelectron sensitivity, $\eta = 0.0021$ is the total detection efficiency including the camera quantum efficiency and the total optical transmission efficiencies, and $R = 1.9 \times 10^{10}$ s^{-1} is the spatially integrated count rate of the CCD. This gives a particle number of $\sim$800 at $P = 1.7P_{\mathrm{th}}$. Combining with the condensate FWHM width of 6 μm, or area of 28 μm^2, gives a density of 3.5×10^8 cm^{-2}. This is much lower than densities at which saturation occurs.

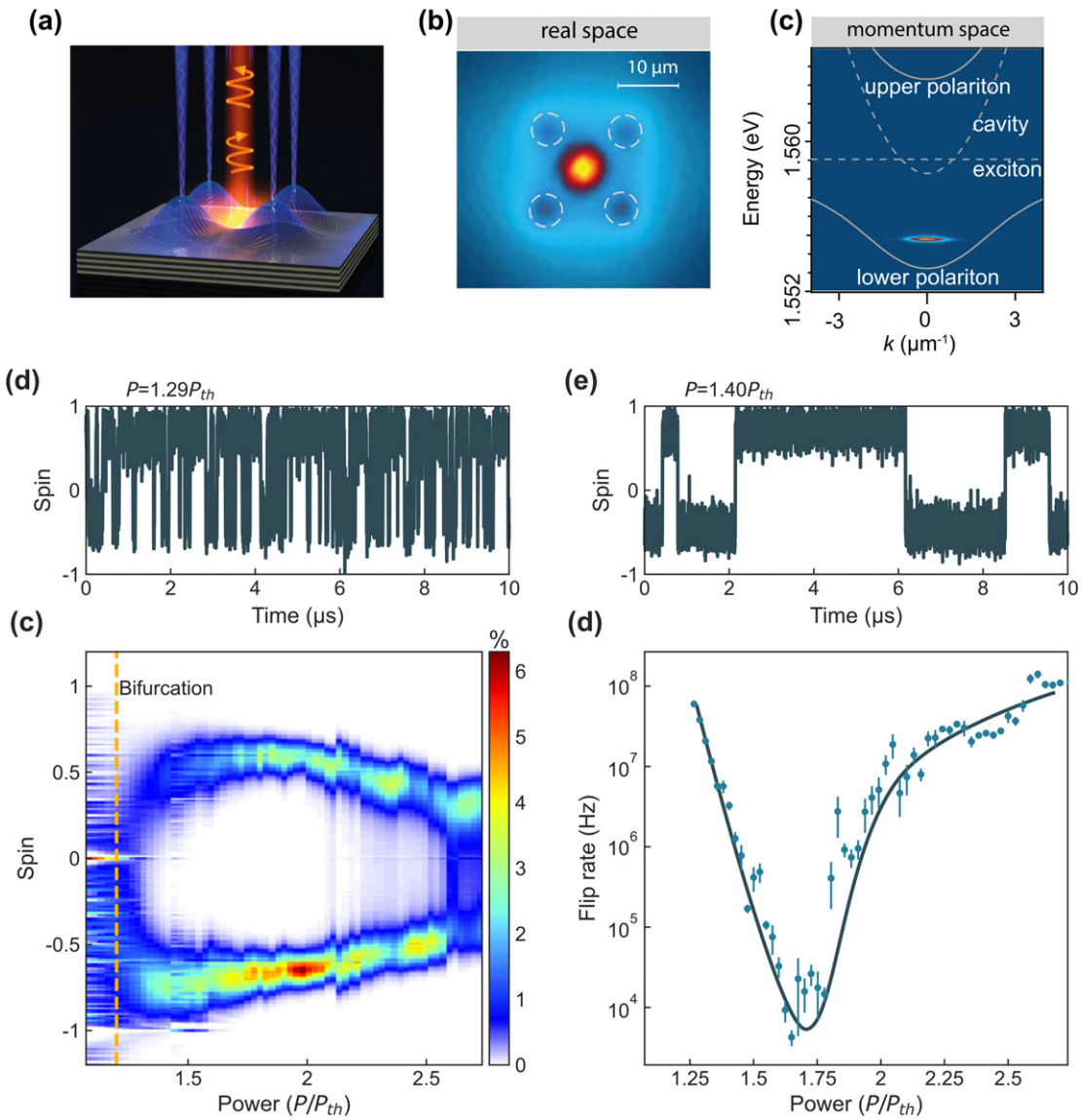

Figure 1. (a) Microcavity excitation configuration, gives (b) real-space coherent condensate emission (pump spots marked by dashed white circles) and (c) momentum space strong-coupling condensate above threshold, which is blueshifted from the lower polariton branch due to polariton nonlinearities. (d), (e) Example spin time traces showing (d) fast and (e) slow flip rates. (f) 2D probability density of spin versus power, extracted from 10 experimental realisations. Larger spin noise at low powers ($<1.3\,P_{\rm th}$) arises from weak emission just above condensation threshold ($P_{\rm th}$). (g) Extracted flip rate versus pump power. Solid line is a guide to the eye. (b,c) modified from [19].

orders of magnitude. This is followed however by a slow increase over a similar range. These trends match the increase and decrease of the spin amplitudes seen in figure 1(f).

Our experiments are limited by the PMT rise time to measuring spin-flip rates below 0.5 GHz, but as we will see later, our simulations show that GHz flip rates can be exceeded. Additionally, we have previously experimentally demonstrated stable circularly-polarised condensates that remain in the same spin for seconds at a time [19], giving us a 9 order-of-magnitude range over which we can optically control the spin-flip rate.

The initial fast decrease of the flip rate (figure 1(g)) and the fast increase of the spin magnitude (figure 1(f)) can be understood phenomenologically within the physics of spin bifurcation [19]. Just after the bifurcation threshold, the two new circularly-polarised states which have small spin magnitudes are easily destabilised and random noise easily initiates flips. The influence of noise decreases as the power increases and the two spin states move further away from each other on the Poincare sphere. However, neither the decrease in the magnitude of the spin nor the increase of the flip rate at higher powers can be explained within previous models of polariton condensation and require new physics to be considered, as we show below.

3. Cross-spin reservoir scattering

To fully account for the spin degree of freedom, we extend previous models of polariton condensates coupled to an exciton reservoir [22, 27]. We consider a spinor exciton reservoir, where each spin component of the reservoir can feed the polariton condensate of the same spin (s) or the opposite spin (o), with two different rates R_s and R_o, respectively:

$$\begin{aligned}
\frac{\mathrm{d}n_+}{\mathrm{d}t} &= P - Gcy_x n_+ - R_s\,|\psi_+|^2 n_+ - R_o\,|\psi_-|^2 n_+,\\
\frac{\mathrm{d}n_-}{\mathrm{d}t} &= P - Gcy_x n_- - R_s\,|\psi_-|^2 n_- - R_o\,|\psi_+|^2 n_-,\\
\frac{\mathrm{d}\psi_+}{\mathrm{d}t} &= \left[\frac{1}{2}(R_s n_+ + R_o n_- - Gcy_p) - \frac{\mathrm{i}}{2}(\alpha_1\,|\psi_+|^2 + \alpha_2\,|\psi_-|^2)\right]\psi_+ - \frac{1}{2}(\gamma - \mathrm{i}\varepsilon)\psi_-\\
&\qquad + \sqrt{R_s n_+ + R_o n_-}\,\frac{\mathrm{d}W_+}{\mathrm{d}t},\\
\frac{\mathrm{d}\psi_-}{\mathrm{d}t} &= \left[\frac{1}{2}(R_s n_- + R_o n_+ - Gcy_p) - \frac{\mathrm{i}}{2}(\alpha_1\,|\psi_-|^2 + \alpha_2\,|\psi_+|^2)\right]\psi_- - \frac{1}{2}(\gamma - \mathrm{i}\varepsilon)\psi_+\\
&\qquad + \sqrt{R_s n_- + R_o n_+}\,\frac{\mathrm{d}W_-}{\mathrm{d}t}\,,
\end{aligned} \tag{1}$$

where $n_{+/-}$ are the number densities of spin up/down exciton reservoirs, $\psi_{+/-}$ are the spin up/down components of the condensate wavefunction, and P is the pumping rate. The values of exciton linewidth (Γ_x), polariton linewidth (Γ_p), and energy (ε) and dissipation (γ) difference between horizontal and vertical polarisation are spectroscopically measured on our specific sample [19], while same-spin (α_1) and cross-spin (α_2) nonlinearities have been measured for similar samples [30]. The last term accounts for fluctuations due to the pumping, with $\mathrm{d}W_\pm$ being two independent complex Gaussian random variables with $\langle \mathrm{d}W_\pm^* \mathrm{d}W_\pm \rangle = \mathrm{d}t$, where $\mathrm{d}t$ is the time step [20, 22, 23]. We consider the case where overlap between condensate and exciton reservoirs is small and hence nonlinearities due to the reservoirs have been neglected.

We work in a regime where the exciton reservoir dynamics are much faster than those of the polaritons [22] and the reservoir occupations adjust adiabatically to the condensate occupation, leading to:

$$n_\pm = \frac{P}{\Gamma_x + R_s\,|\psi_\pm|^2 + R_o\,|\psi_\mp|^2}. \tag{2}$$

Previous work has generally worked in limiting cases of equation (1), assuming that R_o was sufficiently small to be neglected [31, 32], or assuming that cross-scattering into biexcitons was the main process so that $R_s = 0$ [33], or simply assuming $R_o/R_s = 1$ [19, 23]. None of these limiting assumptions are able to explain the results presented here. We note that equation (1) is phenomenological and does not capture the precise details of microscopic scattering processes described elsewhere [30, 32, 34, 35]. The cross-spin scattering (R_o) presented here cannot be used to directly extract the exciton–polariton scattering constants. Nevertheless, equation (1) still provides a qualitative prediction for the experimental spin flip rates, confirming that the value of cross-spin scattering between polariton condensates cannot simply be assumed in phenomenological models.

We simulate the spin dynamics of equation (1) using a 4th order Runge–Kutta numerical solver evolving over 1 μs, for 10 different realisations with random initial conditions. From these time-resolved spin traces (figures 2(a), (b)), we observe that as the power is increased, there is a clear bifurcation from a linearly-polarised state to two circularly polarised states with rapidly increasing magnitude of spin (figure 2(c)). This is followed by a slow decrease of the magnitude of the spin of the two circularly polarised states, in close similarity with experimental data (figure 1(f)). The widening of the lines after $P \sim 2P_{\mathrm{th}}$ does not agree with our experiment but, as we will see later, the widening is due to spin oscillations at rates faster than the 2 ns resolution of our experimental setup.

Another difference between the simulations and the experiment is that the maximum condensate spin for the simulations (0.9 in figure 2(c)) is higher than in experiment (0.6 in figure 1(c)). There are two reasons for this. First, the noise level of the high speed PMTs (~20%) reduces the measured degree of polarisation. Secondly, the maximum spin is equal to the ratio between the energy (ε) and dissipation (γ) splittings [19], which cannot be directly measured. Optimisation of these parameters in the simulations is computationally very costly and will be the subject of future work.

The spin-flip rates extracted from our simulations (figure 2(d)) match the experimental data (figure 1(e)) very well. Using the ratio of cross- to co-spin scattering as the only adjustable parameter, and keeping the total scattering rate $R_o + R_s$ constant, we find qualitative agreement when $R_o/R_s \sim 0.6$. Hence the cross-spin channel does give significant scattering, but is only about half the rate of the same-spin channel. We note obtaining

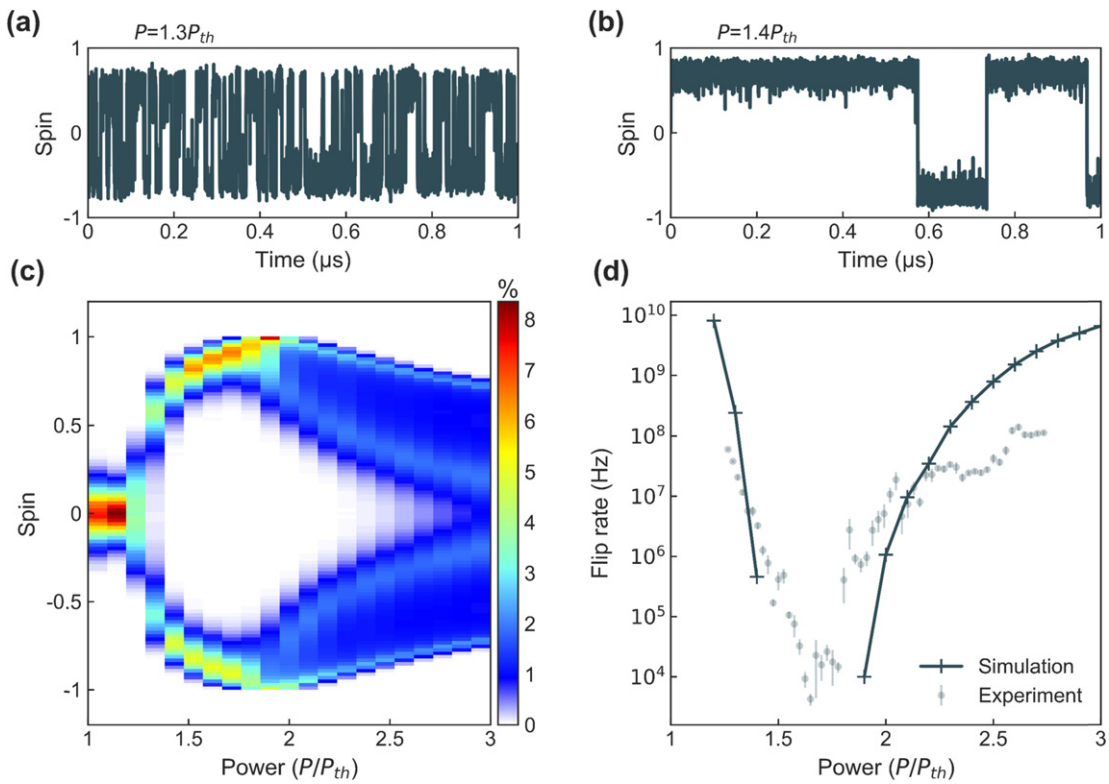

Figure 2. Example spin traces from model showing (a) slow and (b) fast flip rates. (c) 2D probability density of spin versus power. (d) Extracted flip rate versus power. No spin flips were observed between $1.5P_{\rm th}$ and $1.8P_{\rm th}$ for the simulated time ranges. Parameter values: $\Gamma_x = 0.1$ ps^{-1}, $\Gamma_p = 1$ ps^{-1}, $\alpha_1 = 0.01$ ps^{-1}, $\alpha_2 = -0.005$ ps^{-1}, $\varepsilon = 0.1$ ps^{-1}, $\gamma = 0.01$ ps^{-1}, $R_s = 0.1225$ ps^{-1}, $R_o = 0.0775$ ps^{-1}.

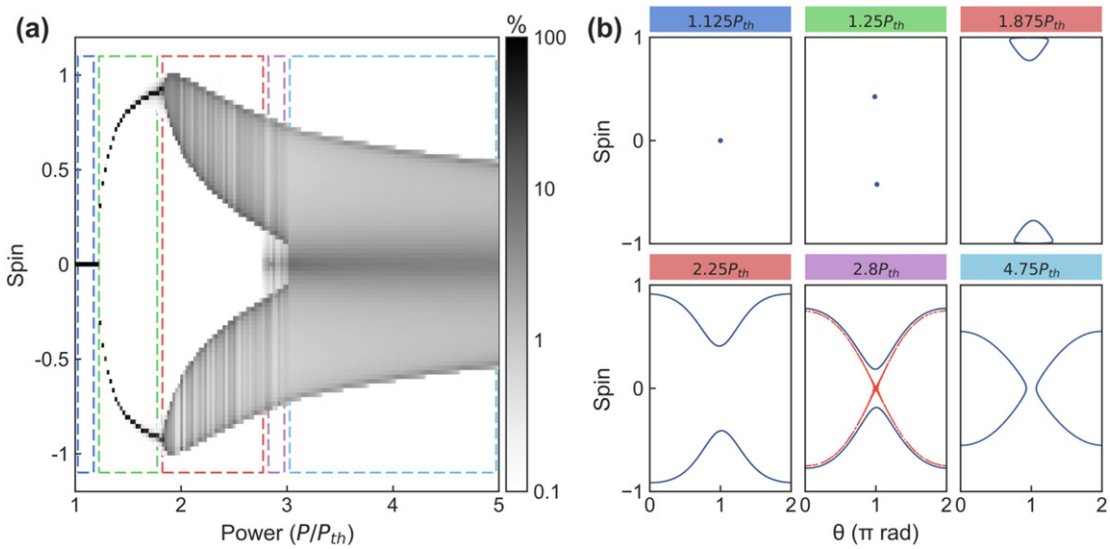

Figure 3. (a) 2D probability density of spin versus power. Dashed rectangular regions mark linearly-polarised (blue), spin-bifurcation (green), limit cycle (red), chaotic (purple), and period-doubling (cyan) phases. (b) Flattened surface of the Poincare sphere: vertical is z-coordinate in Poincare space (degree of circular polarisation), while horizontal corresponds to azimuthal angle (direction of linear polarisation component).

improved agreement at higher powers would require higher time-resolution which is experimentally problematic (see below).

A better qualitative understanding of these phenomena emerges when looking at the solutions in the absence of noise and for a larger range of pumping powers than are easily accessible experimentally (figure 3). Plotting the flattened surface of the Poincare sphere (figure 3(b)) makes it possible to visualise the full dynamics of the

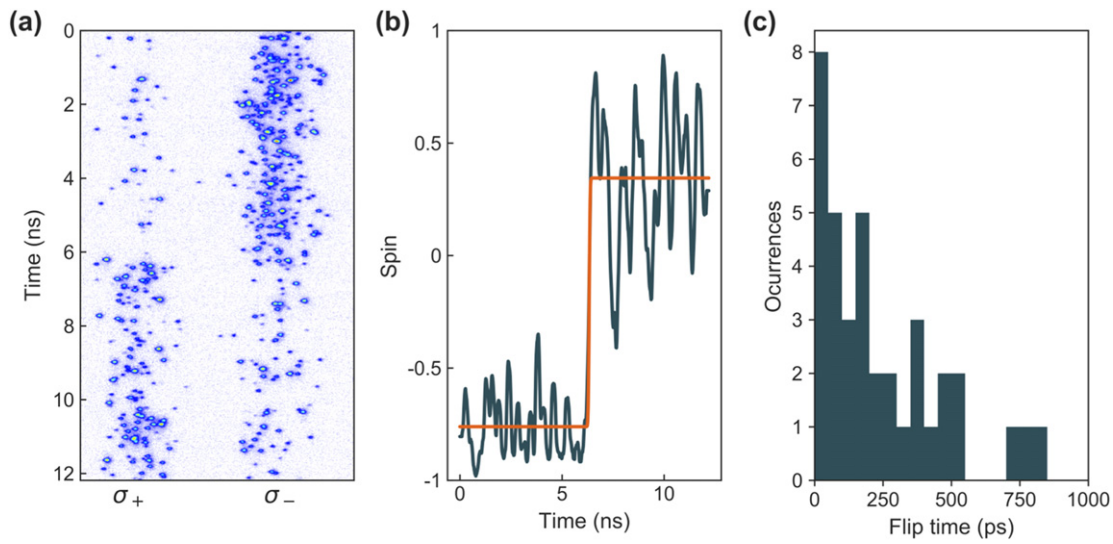

Figure 4. Raw streak image showing single-photon events (a) and extracted spin trace (b) of an ultrafast flip with duration 52 $\pm$ 1 ps (c) histogram of fitted flipping duration times.

spin. As before, with increasing power a single linearly-polarised state ($P = 1.125P_{\text{th}}$) splits into two circularly polarised states ($P = 1.25P_{\text{th}}$), which rapidly develop strong circular polarisation, moving towards the poles of the Poincare sphere. Further increase of the pump power leads to the two circularly polarised steady states turning into limit cycles ($P = 1.875P_{\text{th}}$) through a Hopf bifurcation. These oscillations have periods of ~30 ps, faster than can be experimentally detected, explaining the apparent broadening of the steady states seen in the simulations (figure 2(a)) but not in the experiment (figure 1(a)). With increasing power, the oscillations increase in amplitude ($P = 2.25P_{\text{th}}$) until they merge ($P = 2.8P_{\text{th}}$, red line) into a single attractor around a linearly-polarised state ($P = 4.75P_{\text{th}}$). At the merging of the two limit cycles there are indications of chaotic behaviour (to be treated elsewhere).

This phase diagram (figure 3(a)) can be qualitatively understood as a hierarchical succession of different terms dominating the dynamics in equation (1). Immediately after the parity-breaking bifurcation, the energy (ε) and dissipation (γ) difference between linear modes, and the nonlinearity asymmetry ($\alpha = \alpha_1 - \alpha_2$), lead to stable, almost circularly-polarised fixed-point steady states. As the power is increased, γ becomes negligible and the system undergoes a Hopf bifurcation into effectively conservative spin dynamics. The only relevant terms become ε and α, with the two limit cycle solutions corresponding to self-trapping of two coupled condensates [23, 36]. As the power is further increased, α becomes less and less important (compared to the dissipation nonlinearities), and the self-trapping solutions are destabilised until effectively linear and conservative spin dynamics are obtained, with oscillations around the lowest energy linearly-polarised mode governed by ε.

Using this understanding of the solutions of equation (1) gives a simpler explanation for the experimental power dependence of the flip rate. At the bifurcation, two circularly polarised states are formed very close to each other, and noise from the feeding of polaritons can easily kick the condensate from one state to the other and induce a spin flip. As the power is increased, the two states move away from each other in polarisation space, quickly developing a strong degree of circular polarisation, and making it harder for noise to induce spin flips. This scenario reverses as the two steady states turn into limit cycles with amplitude that slowly increases as we increase the power: the two states come closer together, allowing noise to start inducing spin flips again.

4. Sub-50 ps spin flips

To further understand the dynamics of the system, the speed of individual spin flips is measured using single-shot imaging on a streak camera. While the maximum time resolution of the streak in synchroscan mode is 2 ps, the comparatively smaller signal-to-noise in these single shot images results in a time resolution of 20 ps. We work at a pump power with a small flip rate to be able to easily identify individual spin flips.

Raw streak images (figure 4(a)) clearly reveal spin flips, here with a measured flip time of 52 $\pm$ 1 ps. This is estimated by fitting an error function to the horizontally-binned spin trace (figure 4(b)), and extracting the time taken to go from 10% to 90% of the full spin flip (the standard deviation is extracted from the fitting). Repeating this procedure for many well-isolated spin flips gives histograms of the spin flip times (figure 4(c)).

We observe that 20% of spin flips occur on timescales (<50 ps) comparable to the polariton lifetime (7 ps), as well as a significant number of spin flips that appear to take significantly longer times (though these may also arise from multiple flips or oscillations that cannot be time-resolved). The spin dynamics of the system are governed by the nonlinear interactions which, above threshold, can be faster than the polariton lifetime and have been used to create ultrafast memory devices [37]. The direct single-shot observation of stochastic spin flipping presented here provides a new tool to probe these macroscopic quantum systems, as well as showcase their capability for RNG devices.

5. Conclusion and discussion

We studied the influence of pump power on the stability of spin-bifurcated trapped polariton condensates. We observed a variation of the spin-flip rate by more than four orders of magnitude and an extreme non-monotonous dependence on pump power. We mapped the spin-power phase diagram of the condensate and found that this non-monotonous behaviour is rooted in the asymmetric cross-spin to same-spin scattering between polaritons and reservoir excitons. Qualitative agreement between simulations and experiment was found for ratios of cross-/co-spin scattering ~0.6, in contrast with the literature values where it has generally been assumed to be 0 or 1. These values do not correspond to the scattering constants of excitons, but rather to the values required in the phenomenological model to achieve agreement with experiment. Our simulations also predicted the existence of self-sustained polarisation oscillations, never previously identified for non-resonantly pumped polariton condensates. We time-resolved individual spin flips using single-shot streak camera imaging, and measure flips faster than 50 ps. This indicates that polariton condensates can easily compete with state-of-the-art RNGs based on laser diodes [28].

We note that the non-monotonous behaviour of flip rate with power reported here contrasts with laser diode systems, where noise-driven transitions between steady states increase with increasing power, and the focus has been on polarization chaos and its applications to random number generation [26, 28]. In this context, our work paves the way for a polariton RNG that can be easily parallelised by creating multiple disconnected trapped condensates on the same chip. It would also be interesting to study how the spin-power phase diagram reported here may change in the case of Josephson-coupled pairs [17], and spin lattices of polariton condensates [18].

Acknowledgments

We acknowledge Grants No. EPSRC EP/L027151/1, ERC LINASS 320503, Leverhulme Trust Grant No. VP1-2013-011 and bilateral Greece-Russia 'Polisimulator' project co-financed by Greece and the EU Regional Development Fund. PS acknowledges Saint-Petersburg State University research grant 11.34.2.2012 and AENAO project co-financed by the European Union ERDF and Greek national NSRF 2014-2020 funds. ST acknowledges financial support from the Stavros Niarchos Foundation, 'ARCHERS' project. AJR acknowledges support of Horizon 2020 programme (No. FETPROACT-2016 732894-HOT). YGR acknowledges support from CONACYT (Mexico) grant No. 251808 and by the Institute for Basic Science in Korea (IBS-R024-D1).

ORCID iDs

Yago del Valle-Inclan Redondo https://orcid.org/0000-0003-0886-7226
Hamid Ohadi https://orcid.org/0000-0001-6418-111X
Yuri G Rubo https://orcid.org/0000-0002-5016-2249
Pavlos G Savvidis https://orcid.org/0000-0002-8186-6679
Jeremy J Baumberg https://orcid.org/0000-0002-9606-9488

References

[1] Kavokin A V, Baumberg J J, Malpuech G and Laussy F P 2017 *Microcavities* (Oxford: Oxford University Press)
[2] Kasprzak J *et al* 2006 Bose–Einstein condensation of exciton polaritons *Nature* **443** 409–14
[3] Carusotto I and Ciuti C 2013 Quantum fluids of light *Rev. Mod. Phys.* **85** 299–366
[4] Sanvitto D and Kéna-Cohen S 2016 The road towards polaritonic devices *Nat. Mater.* **15** 1061–73
[5] Liew T C H, Shelykh I A and Malpuech G 2011 Polaritonic devices *Physica* E **43** 1543–68
[6] Balili R, Hartwell V, Snoke D, Pfeiffer L and West K 2007 Bose–Einstein condensation of microcavity polaritons in a trap *Science* **316** 1007–10
[7] Bajoni D, Senellart P, Wertz E, Sagnes I, Miard A, Lemaître A and Bloch J 2008 Polariton laser using single micropillar GaAs-GaAlAs semiconductor cavities *Phys. Rev. Lett.* **100** 047401
[8] Kim N Y *et al* 2008 GaAs microcavity exciton–polaritons in a trap *Phys. Status Solidi* b **245** 1076–80

[9] Cerda-Méndez E A *et al* 2010 Polariton condensation in dynamic acoustic lattices *Phys. Rev. Lett.* **105** 116402
[10] Dreismann A *et al* 2016 A sub-femtojoule electrical spin-switch based on optically trapped polariton condensates *Nat. Mater.* **15** 1074–8
[11] Sanvitto D *et al* 2011 All-optical control of the quantum flow of a polariton condensate *Nat. Photon.* **5** 610–4
[12] Amo A *et al* 2009 Collective fluid dynamics of a polariton condensate in a semiconductor microcavity *Nature* **457** 291–5
[13] Hayat A *et al* 2012 Dynamic Stark effect in strongly coupled microcavity exciton polaritons *Phys. Rev. Lett.* **109** 033605
[14] Cristofolini P, Dreismann A, Christmann G, Franchetti G, Berloff N G, Tsotsis P, Hatzopoulos Z, Savvidis P G and Baumberg J J 2013 Optical superfluid phase transitions and trapping of polariton condensates *Phys. Rev. Lett.* **110** 186403
[15] Askitopoulos A, Ohadi H, Kavokin A V, Hatzopoulos Z, Savvidis P G and Lagoudakis P G 2013 Polariton condensation in an optically induced two-dimensional potential *Phys. Rev.* B **88** 041308
[16] Askitopoulos A, Liew T C H, Ohadi H, Hatzopoulos Z, Savvidis P G and Lagoudakis P G 2014 Robust platform for engineering pure-quantum-state transitions in polariton condensates *Phys. Rev.* B **92** 035305
[17] Ohadi H, del Valle-Inclan Redondo Y, Dreismann A, Rubo Y G, Pinsker F, Tsintzos S I, Hatzopoulos Z, Savvidis P G and Baumberg J J 2016 Tunable magnetic alignment between trapped exciton–polariton condensates *Phys. Rev. Lett.* **116** 106403
[18] Ohadi H *et al* 2017 Spin order and phase transitions in chains of polariton condensates *Phys. Rev. Lett.* **119** 067401
[19] Ohadi H, Dreismann A, Rubo Y G, Pinsker F, del Valle-Inclan Redondo Y, Tsintzos S I, Hatzopoulos Z, Savvidis P G and Baumberg J J 2015 Spontaneous spin bifurcations and ferromagnetic phase transitions in a spinor exciton–polariton condensate *Phys. Rev.* X **5** 031002
[20] Rubo Y G 2004 Kinetics of the polariton condensate formation in a microcavity *Phys. Status Solidi* a **201** 641–5
[21] Wouters M and Savona V 2009 Stochastic classical field model for polariton condensates *Phys. Rev.* B **79** 165302
[22] Wouters M, Carusotto I and Ciuti C 2008 Spatial and spectral shape of inhomogeneous nonequilibrium exciton–polariton condensates *Phys. Rev.* B **77** 115340
[23] Read D, Liew T C H, Rubo Y G and Kavokin A V 2009 Stochastic polarization formation in exciton–polariton Bose–Einstein condensates *Phys. Rev. B* **80** 195309
[24] Ohadi H, Kammann E, Liew T C H, Lagoudakis K G, Kavokin A V and Lagoudakis P G 2012 Spontaneous symmetry breaking in a polariton and photon laser *Phys. Rev. Lett.* **109** 016404
[25] Baumberg J *et al* 2008 Spontaneous polarization buildup in a room-temperature polariton laser *Phys. Rev. Lett.* **101** 136409
[26] Virte M, Panajotov K, Thienpont H and Sciamanna M 2013 Deterministic polarization chaos from a laser diode *Nat. Photon.* **7** 60–5
[27] Wouters M and Carusotto I 2007 Excitations in a nonequilibrium Bose–Einstein condensate of exciton polaritons *Phys. Rev. Lett.* **99** 140402
[28] Sciamanna M and Shore K A 2015 Physics and applications of laser diode chaos *Nat. Photon.* **9** 151–62
[29] Tsotsis P, Eldridge P S, Gao T, Tsintzos S I, Hatzopoulos Z and Savvidis P G 2012 Lasing threshold doubling at the crossover from strong to weak coupling regime in GaAs microcavity *New J. Phys.* **14** 023060
[30] Takemura N, Trebaol S, Wouters M, Portella-Oberli M T and Deveaud B 2014 Heterodyne spectroscopy of polariton spinor interactions *Phys. Rev.* B **90** 195307
[31] Borgh M O, Keeling J and Berloff N G 2010 Spatial pattern formation and polarization dynamics of a nonequilibrium spinor polariton condensate *Phys. Rev.* B **81** 235302
[32] Ciuti C, Savona V, Piermarocchi C, Quattropani A and Schwendimann P 1998 Role of the exchange of carriers in elastic exciton–exciton scattering in quantum wells *Phys. Rev.* B **58** 7926–33
[33] Wouters M, Paraïso T K, Léger Y, Cerna R, Morier-Genoud F, Portella-Oberli M T and Deveaud-Plédran B 2013 Influence of a nonradiative reservoir on polariton spin multistability *Phys. Rev.* B **87** 045303
[34] Vladimirova M *et al* 2010 Polariton–polariton interaction constants in microcavities *Phys. Rev.* B **82** 075301
[35] Shelykh I A, Kavokin A V, Rubo Y G, Liew T C H and Malpuech G 2010 Polariton polarization-sensitive phenomena in planar semiconductor microcavities *Semicond. Sci. Technol.* **25** 013001
[36] Raghavan S, Smerzi A, Fantoni S and Shenoy S R 1999 Coherent oscillations between two weakly coupled Bose–Einstein condensates: Josephson effects, π oscillations, and macroscopic quantum self-trapping *Phys. Rev.* A **59** 620–33
[37] Cerna R, Léger Y, Paraïso T K, Wouters M, Morier-Genoud F, Portella-Oberli M T and Deveaud B 2013 Ultrafast tristable spin memory of a coherent polariton gas *Nat. Commun.* **4** 2008